sustainability

MDPI

Article

Influence of Feedstock and Final Pyrolysis Temperature on Breaking Strength and Dust Production of Wood-Derived Biochars

María Videgain [1,*], Joan J. Manyà [2], Mariano Vidal [3], Eva Cristina Correa [4], Belén Diezma [4] and Francisco Javier García-Ramos [1]

1 Instituto Agroalimentario de Aragón—IA2 (CITA-UNIZAR), EPS-Universidad de Zaragoza, E-22071 Huesca, Spain; fjavier@unizar.es
2 Thermochemical Processes Group, Aragón Institute of Engineering Research (I3A), EPS, University of Zaragoza, E-22071 Huesca, Spain; joanjoma@unizar.es
3 Departamento de Ingeniería Mecánica, EPS, University of Zaragoza, E-22071 Huesca, Spain; vidalcor@unizar.es
4 Laboratorio de Propiedades Físicas y Técnicas Avanzadas en Agroalimentación, ETSIAAB, Universidad Politécnica de Madrid, E-28040 Madrid, Spain; evacristina.correa@upm.es (E.C.C.); belen.diezma@upm.es (B.D.)
* Correspondence: mvidegain@unizar.es; Tel.: +34-974292656

Abstract: The susceptibility to fragmentation of biochar is an important property to consider in field applications. Physical and mechanical properties of wood-derived biochars from vine shoots and holm oak were studied to evaluate the effect of biomass feedstock, final pyrolysis temperature and application conditions. Vine shoots and holm oak pruning residues were selected for biochar production. Slow pyrolysis experiments were conducted at two different final temperatures (400 and 600 °C). Physical and chemical characteristics of biomass and biochars were determined. Impact strength was evaluated through the measurement of the gravitational potential energy per unit area (J mm^{-2}) necessary for the breakage of biochar fragments. Shear strength (N mm^{-2}) and a combination of shear/compression strengths (N) were analyzed using a Universal Texture Analyzer. A particular mechanical treatment was carried out on biochar samples to simulate the processing bodies of a commercial manure spreader, under two gravimetric moisture contents. Holm oak-derived biochar was more resistant than vine shoot-derived biochar to the applied forces. Vine shoots-derived biochar did not show a significantly different mechanical behavior between temperatures. Holm Oak-derived biochar produced at the higher final pyrolysis temperature showed higher resistance to be broken into smaller pieces. Moistening resulted in an adequate practice to improve mechanical spreading.

Keywords: physical characterization; mechanical processing; vineyard pruning; holm oak pruning; particulate matter; biochar moistening

Citation: Videgain, M.; Manyà, J.J.; Vidal, M.; Correa, E.C.; Diezma, B.; García-Ramos, F.J. Influence of Feedstock and Final Pyrolysis Temperature on Breaking Strength and Dust Production of Wood-Derived Biochars. *Sustainability* **2021**, *13*, 11871. https://doi.org/10.3390/su132111871

Academic Editors: Simeng Li and Ana Méndez

Received: 28 August 2021
Accepted: 23 October 2021
Published: 27 October 2021

1. Introduction

Wood-derived biochar refers to the carbonaceous solid material resulting from the pyrolysis of wood at relatively low temperatures (<700 °C) in an oxygen-limited atmosphere [1]. Biochar has been widely studied in the last few years, owing to the wide range of agricultural benefits related to its application as an organic amendment (e.g., improvement of soil fertility, contribution to a carbon-negative process [2–5]). Based on the extensive available literature, it can be stated that the benefits of applying biochar on soil ecosystem services are site-specific [6], and they are influenced by the type of biomass used as feedstock [7,8]. Furthermore, the pyrolysis experimental conditions (i.e., final pyrolysis temperature, pressure, heating time and residence time of the gas phase) govern the properties of resulting biochar [9–11]. The application rate [12] and particle

size [13,14] also significantly affect the potential benefits of biochar use as a soil amendment. Ultimately, biochar is a general term that encompasses products of quite different nature and properties; the inclusion of details about its properties in research publications seems to be essential both to establish the most appropriate use and to gain deeper knowledge on this topic [15,16].

Some organizations have developed characterization standards (European Biochar Foundation-EBC [17] and International Biochar Initiative-IBI [1]), whose guidelines describe analytical methods for physical and chemical properties, storage instructions, and application conditions that ensure the quality of potential commercial biochars. In addition to other research works [18–20], these guidelines emphasize about the application conditions and the need to properly prescreening and characterizing the biochar batches after the pretreatments needed for their proper application (i.e., grinding, granulation, moistening, etc.) [21]. There are still technical and practical barriers both for safe handling and large-scale application of biochar [20]. The mechanical stresses resulting from biochar application to soil can favor its release into the atmosphere, specifically contributing to airborne particulate matter < 10 μm in diameter (PM_{10}), which are liable to remain in the air and enter the respiratory tract of humans [22,23]. Anthropogenic Black Carbon aerosols (BCa) have a significant radiative forcing potential and a clear climate warming effect [24]. Fine particles of biochar can also promote the transport of adsorbed contaminants in water by percolation and runoff [25]. In addition, biochar dust is susceptible to ignition when stored in enclosed spaces [20]. Hence, moistening the biochar prior to its soil application is a recommended practice in order to reduce particulate matter emissions [1]. A recommended moisture content is not specified in EBC or IBI guidelines. Silva et al. [26] measured the threshold friction velocities of a range of biochar particles at different moisture contents, and they determined an optimum gravimetric moisture content above 15%. However, biochar resistance to be broken into smaller pieces is governed by mechanical properties of biochar, which so far have not been properly assessed [16].

On the one hand, both penetration resistance and aggregate stability of the soil once biochar is applied are some of the measured parameters [27,28] when the objective is to determine the mechanical properties of the amended soil. On the other hand, the mechanical behavior of biochar has been assessed for specific applications such as land-fill biocovers and in-ground filtration systems [29–31], addition of charcoal to construction materials or biocomposites [32], fuel pellets production [33–35], and heating blast furnaces to industrial iron production [36–39]. The characterization methodologies adopted for the aforementioned applications are based on standards for soils, geoengineering, plastics, and other specific materials. To the best of our knowledge, there are no standardized methods for determining strength properties of biochar related to its soil application, an issue whose standardization would be extremely complex due to the wide range of biomass feedstocks and pyrolysis process conditions, with consequent biochar of very diversified structures and textures.

Several studies showed clear correlations between the properties of the parent material used as biochar feedstock and the mechanical behavior of biochar [40–43]. Furthermore, relying on previous studies, pyrolysis operating conditions play a significant role in the final product behavior, with a general trend of increasing the material resistance with final pyrolysis temperature [37,41,42,44]. Kumar et al. [37] determined—for chars produced from acacia and eucalyptus species—a decrease in crushing and impact strengths with increasing carbonization temperature up to 600 °C, followed by an increase above this temperature. Das et al. [41], via nanoindentation, concluded that a combination of high final pyrolysis temperature (≥500 °C) and relatively long residence time (~60 min) led to an increase in the values of hardness and elastic modulus of seven residues-derived biochars. Nevertheless, the opposite effect was also reported [45] with loss of dynamic hardness with increasing pyrolysis temperature.

The present study aims to assess the influence of feedstock and final pyrolysis temperature on both the particle size distribution of wood-derived biochar and its mechan-

ical behavior through the measurement of shear strength and a combination of forces (shear/compression). A Universal Texture Analyzer was used to test these properties on biochar fragments. The effect of experimental conditions (biomass feedstock and pyrolysis temperature) on biochar particle size distribution was also evaluated by a mechanical process simulating biochar spreading at the soil surface.

2. Materials and Methods

2.1. Biomass Origin and Characterization

Pruning remains from thinning in a scrub area (Clean Cellulosic Biomass [1]) of holm oaks (HO) (*Quercus ilex* L.), and vine shoots pruning residues from the province of Huesca (Spain), were used as biochar feedstocks. The agronomic characteristics of vineyards are detailed in a previous publication [46]. Both pruning remains corresponded to branches of one year of age.

Biomass was selected by diameter (between 5.0 and 10.0 mm) and chopped up using a domestic shredder (ZI-GHAS2800, ZIPPER Maschinen GmbH, Schlüblberg, Austria) into pieces of 20–50 mm in length. These particle sizes were used in order to following a cutting practice that could be carried out under field conditions in a reasonable way. In addition, these particle sizes could enhance the carbonization efficiency of the pyrolysis process [47].

Proximate analyses were performed by following the ASTM standards [48] as it is detailed in a previous publication [46]. X-ray fluorescence (XRF) spectroscopy was used to determine the inorganic elements of biomass, by means of a Niton XL3t GOLD++ portable analyzer (Thermo Fisher Scientific, Waltham, MA, USA). TestAll^{TM} Geo mode was used, with a 120 s acquisition time, and at least three measurements per analysis were conducted.

Van Soest method was adopted to determine the biomass constituents (lignin, cellulose, hemicellulose and extractives) [49]. The complete description of this procedure is available in previous publications [47,50].

EBC methodology [1] was followed to measuring bulk density of three composite samples of biomass and biochar, determining the mass that could be packed into a 20 mL stainless-steel cylinder with minimal compression.

Water holding capacity (WHC) of biochar samples was determined by gravimetry through pressure plates (Richards chambers, −33 kPa–1500 kPa).

2.2. Production of Biochar and Characterization

Slow pyrolysis runs were performed under atmospheric pressure and at two different final pyrolysis temperatures (400 and 600 °C). The average heating rate was 5 °C min^{-1}. A total of 20 experiments were conducted (5 repetitions for each type of feedstock and final pyrolysis temperature). The pyrolysis device and experimental conditions details are reported in previous publications [46,51]. Proximate, elemental and XRF analyses were carried out following the aforementioned methodology. The specific surface area (S_{BET}) was determined using a gas sorption analyzer through the measurements of CO_2 adsorption isotherms at 0 °C. The detailed procedure for S_{BET} determination and pore volume (volume total–V_{total} and ultramicropore–V_{ultra}) is available in a previous publication [47].

The raw biochars were sieved to different sizes to establish the particle size distribution. The amount of biochar retained on each sieve was weighed on a precision balance. Dry sieving was used to separate large fragments (≥2 mm), while wet sieving was applied for the fine fraction (<2 mm, but ≥0.001); the finest particles (<0.010 mm) were retained on filter papers through an in-line filter holder (Sartorius, Goettingen, Germany) connected to a vacuum pump. The fraction of particles < 0.010 mm was calculated as the difference between the fraction measured in 2 mm sieve and the sum of the retained fractions values measured by wet sieving (0.01–2.00 mm). Both the sieves used for the wet sieving and the filter papers were dried prior to the sample retention and subsequently dried in an oven at 70 °C until constant weight. The work was carried out inside an airless extraction hood. The difference between the initial weight of the samples and the sum of the different size fractions was negligible.

Morphological characterization was carried out for three samples (i.e., three different pyrolysis runs) of each type of biochar (or treatment). 10% in weight of the coarse fraction (>2 mm length) was sampled fragment (resulting in 368 and 172 fragments for VS and HO-derived biochars, respectively) and the following measures were performed: length and diameter (digital caliper Twin-Cal IP40, TESA, Renens, Switzerland), mass (precision balance cp224s-Oce, Sartorius, Goettingen, Germany), volume (by displacement of water in a graduate tube [43]), and bulk density of each individual fragment as a quotient between the two latter parameters. The shape coefficient was calculated as the quotient between the measured diameter of each fragment and the equivalent diameter (diameter of a cylinder with equivalent volume).

2.3. Mechanical Behavior

2.3.1. Impact Strength and Texturometer Measurements

The height (within a range from 1 to 3 m) necessary for the breakage of each fragment of biochar onto a metal surface was measured. The mass and the rupture area were determined to calculate the potential breakage energy ($E_p = mgh$) per unit area (J mm^{-2}). A total of 125 fragments of each sample was tested in this experiment.

In a second step, a Universal Texture Analyzer was used to evaluate the rheological behavior of biochar through different measurements. Shear strength (N mm^{-2}) was calculated as the maximum force per unit area that could be applied to a biochar fragment before crushing. It was determined for 30 fragments of each treatment using a texture analyzer TA-XT2 (Stable Micro Systems Ltd., Godalming, UK), a universal machine controlled by specific software. Each fragment of biochar was introduced horizontally in a methacrylate support with a separation of 0.75 cm between the fixed extremes. A central piece is vertically displaced by the load cell exerting the shear stress perpendicular to the fibers of each biochar fragment. The load cell of the texturometer descended at a speed of 3 mm s^{-1}. The unit area on which the force was exerted was calculated as twice the cross-sectional area of the fragment. The same texturometer, with a Kramer shear cell coupled, was used to determine the resistance to a combination of compression and shear strengths (N) exerted parallel to the fibers. This process was undertaken using 5 g of each sample by triplicate. The mass of fine particles (<2 mm) generated as a result of this test was measured. The maximum applied force (N), both for shear strength and Kramer shear cell measurements, was fixed in 25 kg.

2.3.2. Mechanical Simulation of Biochar Spreading and Moistening

A mechanical process was combined with two moisture contents to achieve a factorial design:

- Factor 1: biomass pyrolysis feedstock (VS: vine shoots—HO: Holm oak).
- Factor 2: final pyrolysis temperature (400–600 °C).
- Factor 3: mechanical process (Control: without mechanical processing—P: mechanically processed with the raw moisture content—P15: mechanically processed with 15 wt.% moisture content).

Three replicates were carried out for the 12 resulting samples.

The mechanical processing was carried out using an automatic mechanical agitation system, in which the movement in a manure spreader was reproduced. The constructive scheme is detailed in Figure 1. This process was performed for three biochar samples (i.e., 150 g from each sample) and treatments. The main velocity of the mechanical agitation process was 50 rpm. After processing, particle size distribution was measured following the same methodology as described in Section 2.2. The 15 wt.% moisture content was attained following the same methodology as described by Silva et al. [26].

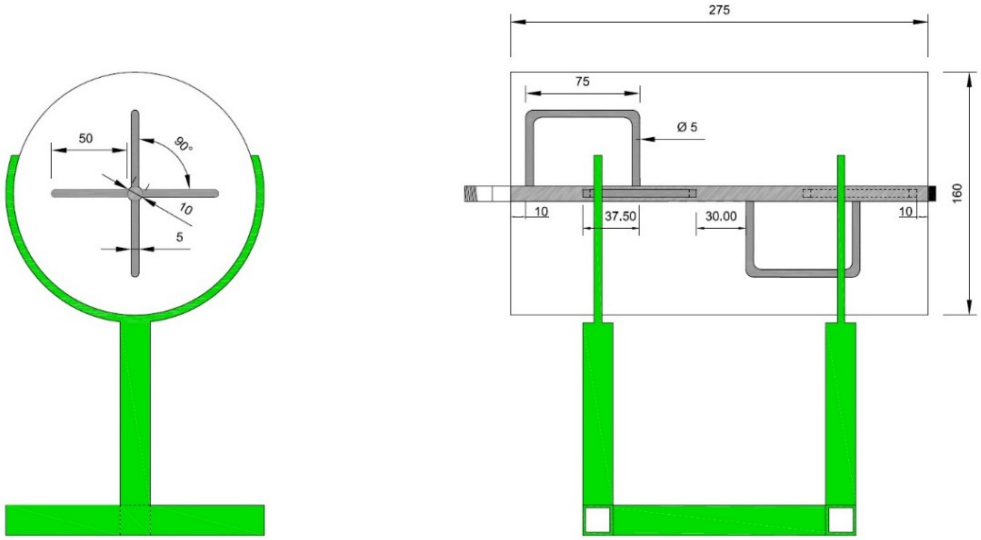

Figure 1. Automatic mechanical agitation system developed to simulate the mechanical spreading. Units: mm.

2.4. Statistical Analysis of Results

IBM SPSS Statistics v.26 (IBM Corp., Armonk, NY, USA) software package was used to perform the statistical analysis of data. Two-way ANOVA was conducted (at a significance level of 0.05) to detect significant differences in the response variables (both physical characterization and texturometer measurements) between the two biochar feedstocks and the two final pyrolysis temperatures, respectively. Three-way ANOVA was conducted to verify the effect of factors (biomass, temperature and mechanical process) and their interactions on the particle size distribution. The comparison between treatment means was performed using the Tukey's method at a significance level of 0.05. The data of particle size distribution (%) were transformed into arcsine for statistical analysis.

3. Results and Discussion

3.1. Biomass and Biochar Characterization

Table 1 details the results from proximate, ultimate, biomass constituents, surface area and porosity, bulk density and product yield fractions determined for both biomass and biochar samples.

Lignin (+silica) content was higher in HO biomass (20.16 and 23.60 wt.% for VS and HO, respectively), according to the different nature of these feedstocks. However, these contents were relatively low in absolute terms. This can be explained by the type of pruning residues selected in the present study, since they come from shoots/branches of one year of age with lower level of lignification than other more developed parts of these plants. It must be pointed out that lignin is the constituent, which mostly contributes to the char yield [53].

Regarding the results from biochar samples, as expected, the higher the final pyrolysis temperature, the larger the fixed carbon content. The nitrogen, oxygen and hydrogen fractions decreased with an increased temperature. Again, calcium was the predominant inorganic element, showing larger concentrations than the previously determined for raw biomass as a consequence of the loss of organic matter during the process. The concentration of inorganic compounds can significantly affect the pyrolysis process. The cracking and polymerization reactions of tar vapors, and the primary devolatilization reactions are influenced by alkali elements (particularly K). In addition to this, the degradation of hemicelluloses could be partly inhibited by the presence of Ca [47].

Table 1. Results from proximate, ultimate, biomass constituents, porosity properties and product yield determined for the feedstocks and/or obtained biochars.

Proximate (wt.% from Triplicate)	**VS**	**HO**		**VS400**	**VS600**	**HO400**	**HO600**
Ash (dry basis)	2.75 ± 0.34	3.55 ± 1.08		6.49 ± 0.14	10.34 ± 0.81	8.28 ± 0.17	11.54 ± 0.49
Moisture	10.47 ± 0.11	7.48 ± 0.07		0.57 ± 0.22	0.72 ± 0.34	0.38 ± 0.01	0.88 ± 0.12
Volatile matter (dry basis)	81.46 ± 2.35	77.86 ± 2.83		22.17 ± 0.01	2.47 ± 0.71	25.22 ± 0.06	7.38 ± 0.21
Fixed Carbon (dry basis)	15.79 ± 1.13	18.59 ± 1.99		71.34 ± 6.45	87.20 ± 1.32	66.50 ± 3.61	81.07 ± 2.52
Elemental (wt.% in daf [1] basis from triplicate) [2]							
C	42.29 ± 0.49	46.2 ± 0.54		71.50 ± 0.48	82.89 ± 0.33	63.76 ± 0.32	72.74 ± 0.01
H	5.24 ± 0.06	8.16 ± 0.07		4.46 ± 0.19	1.95 ± 0.08	3.86 ± 0.05	2.30 ± 0.07
N	13.52 ± 0.35	9.21 ± 0.16		1.58 ± 0.10	1.52 ± 0.01	0.93 ± 0.01	0.74 ± 0.04
O	38.96 ± 0.45	36.43 ± 0.22		22.42 ± 0.77	13.63 ± 0.31	31.67 ± 0.27	24.20 ± 0.11
Elemental inorganic matter (wt.% from triplicate) [3]							
Ca	1.13 ± 0.40	2.64 ± 0.40		2.61 ± 0.32	3.02 ± 0.39	4.30 ± 0.12	7.50 ± 0.62
Si	0.47 ± 0.03	0.69 ± 0.32		0.31 ± 0.05	0.24 ± 0.01	0.61 ± 0.01	0.41 ± 0.06
K	0.38 ± 0.15	0.19 ± 0.01		1.48 ± 0.18	4.29 ± 0.52	0.63 ± 0.02	0.95 ± 0.04
S	0.21 ± 0.06	0.17 ± 0.02		0.13 ± 0.03	0.40 ± 0.03	0.15 ± 0.02	0.12 ± 0.01
Al	0.09 ± 0.01	0.15 ± 0.12		0.03 ± 0.00	0.16 ± 0.01	0.19 ± 0.01	0.06 ± 0.00
Mg	0.11 ± 0.00	0.12 ± 0.01		0.31 ± 0.01	0.45 ± 0.02	0.58 ± 0.04	0.41 ± 0.02
P	0.21 ± 0.02	0.07 ± 0.01		0.27 ± 0.02	1.01 ± 0.07	0.26 ± 0.02	0.15 ± 0.02
Fe	0.03 ± 0.01	0.05 ± 0.03		0.02 ± 0.00	0.03 ± 0.01	0.13 ± 0.01	0.10 ± 0.02
Lignocellulosic constituents and extractives (wt.% from triplicate)			**Surface area and pore volume**				
Lignin + silica	20.16 ± 0.49	23.60 ± 0.54	S_{BET} (m^2 g^{-1})	105.80	227.50	122.30	232.79
Cellulose	34.18 ± 1.95	36.90 ± 0.50	V_{total} (cm^3 g^{-1})	0.0370	0.0819	0.0430	0.0930
Carbohydrate + protein	33.02 ± 0.18	29.03 ± 1.12	V_{ultra} (cm^3 g^{-1})	0.0361	0.0816	0.0428	0.0858
Hemicellulose + acid soluble ash	8.10 ± 1.63	7.25 ± 1.44	**Product yield (-) (n = 5)**				
Extractives	4.54 ± 0.05	3.22 ± 0.09	y_{char}	0.38 ± 0.02	0.29 ± 0.01	0.41 ± 0.03	0.30 ± 0.01
Bulk density (g cm^{-3} from triplicate)	0.35 ± 0.05	0.86 ± 0.08		0.25 ± 0.06	0.23 ± 0.04	0.55 ± 0.12	0.51 ± 0.08
Water Holding capacity (wt.% from triplicate)				14.16 ± 1.25	18.35 ± 1.36	4.56 ± 0.79	13.66 ± 1.11

[1] Dry-ash-free. [2] Oxygen is calculated by difference. [3] Only listed components with a composition higher than 0.01%. VS: Vine Shoots; HO: Holm Oak; 400/600: final pyrolysis temperature of biochar-°C. Values are presented as mean ± standard deviation. Regarding the raw biomasses, results from proximate, elemental and inorganic matter are consistent with previous publications [10,46,52], with slight differences between both types of biomass. The ash content was higher in HO than VS, probably related to the presence of leaves in HO pruning residues. It should be highlighted the relatively large amount of calcium measured, especially for HO biomass.

From the results of bulk density, measured in composite samples through the stainless-steel cylinder method, HO showed higher bulk density than VS (0.86 and 0.35 g cm^{-3} respectively). This difference was maintained in bulk density determinations for biochar samples, although with slightly higher values from biochars produced at lower final pyrolysis temperatures.

Both pore volume and S_{bet} increased with final pyrolysis temperature. Higher porous structures are developed due to the removal of Oxygen and hydrogen during the de-volatilization process. The same trend was observed in WHC values. VS-derived biochar showed higher general values for WHC than HO biochar. It was consistent with bulk density results, despite the S_{bet} and pore volume values of VS biochar being slightly lower than HO biochar. An in-depth study of the pore structure and the correlation for both types of biochar could help to understand these results. HO400 showed a particularly low WHC value (4.56 wt.% versus a mean value of 15 wt.% in the other samples). This may be related to the low fixed carbon content (and high volatile matter content and density) determined for this biochar.

Results from physical characterization of the biochar fragments are shown in Table 2.

Table 2. Influence of feedstock and final pyrolysis temperature on physical properties of the produced biochars.

Parameter	VS400	VS600	HO400	HO600
M (g)	0.32 ± 0.15 c	0.29 ± 0.13 c	0.92 ± 0.17 b	0.97 ± 0.29 a
L (mm)	43.08 ± 9.55 ab	41.38 ± 8.81 b	45.17 ± 6.52 a	45.67 ± 7.83 a
V (cm^3)	0.99 ± 0.34 c	0.80 ± 0.31 d	1.65 ± 0.41 b	1.84 ± 0.52 a
Ø (mm)	4.58 ± 1.02 b	4.50 ± 1.00 b	7.37 ± 1.18 a	7.28 ± 0.95 a
Shape coefficient (-)	0.86 ± 0.16 c	0.93 ± 0.17 b	0.96 ± 0.11 a	0.98 ± 0.14 a
Bulk density (g cm^{-3})	0.33 ± 0.11 d	0.38 ± 0.16 c	0.56 ± 0.05 b	0.53 ± 0.09 a

Different letters within a row denote statistically significant differences ($p < 0.05$) between the biochar samples (Tukey's test). Values are presented as mean ± standard deviation. VS: Vine Shoots; HO: Holm Oak; 400/600: final pyrolysis temperature of biochar-°C.

Feedstock was found to be the main effect influencing all the physical properties of biochars ($p < 0.0001$). Mass was also significantly affected by pyrolysis temperature ($p < 0.0001$). In addition, all the variables were significantly affected by the interaction of the two factors. Biochar from VS featured fragments with lower values of mass (0.32 and 0.29 g for VS400 and VS600, respectively) and average values of approx. 42.2 mm in length. HO fragments showed higher values of mass (0.92 and 0.97 for HO400 and HO600, respectively) and an average value of approx. 45.4 mm in length. The volume of VS600 was significantly lower than that of VS400, while the behavior for HO biochar was the opposite. The measured diameters did not show significant differences as a function of pyrolysis temperature (for a given feedstock) and, therefore, the shape coefficients were relatively high and homogeneous.

Bulk density is one of the most important properties to consider for field application, both due to the importance of knowing the units of elements that are applied into the soil, and the need to regulate the machinery for its application. The results obtained from bulk density through the two different methodologies adopted for composite samples and fragments varied considerably for the VS-derived biochar. This could be related to an underestimation of the volume measured under the immersion method. Different methodologies developed to measure skeletal density through helium pycnometry combined with the determination of envelope density by displacement of a dry granular suspension [54] could be more suitable for this purpose. In addition, an in-depth study on the hydrophobicity of both types of biochar analyzed could help to understand the different behavior showed for VS and HO biochar, since the values of HO biochar were close between the two methods.

Physical characterization confirmed the different type of product to be handled in field applications, due to both the nature of feedstock and final pyrolysis temperature. These biochar characteristics allow one to select the type of machinery for its appropriate application.

3.2. Strength Measurements

From the results obtained in impact tests, a contingency table was built (see Table 3). From the table, it can be seen that none of the HO biochar fragments broke due to the impact at a maximum drop height of 3 m. Regarding VS biochar, no significant differences were detected between pyrolysis temperatures for the percentage of fragments that suffered breakage.

Table 3. Impact test results.

Sample	Break	No Break	χ^2	Breaking Ep (J mm^{-2})	*p*-Value
VS400	70.4%	29.6%	0.143	0.20 ± 0.09	0.648
VS600	77.1%	22.9%		0.22 ± 0.11	
HO400	0%	100%			
HO600	0%	100%			

VS: Vine Shoots; HO: Holm Oak; 400/600: final pyrolysis temperature of biochar-°C.

The number of pieces (mean value + SD) in which each fragment broke into was 2.10 ± 0.04 and 2.20 ± 0.03 for VS400 and VS600, respectively. Difference was not statistically significant.

Regarding the effect of final pyrolysis temperature on the breaking gravitational potential energy per unit area required to break the VS biochar samples, the mechanical behavior between VS400 and VS600 were statistically similar (see Table 3) with an average value of 0.21 ± 0.16 J mm^{-2}.

Figure 2 shows the results obtained for shear strength (N mm^{-2}) and Kramer cell force (N) as a function of both biomass feedstock and final pyrolysis temperature. Results from two-way ANOVA revealed a clear effect of biomass type ($p < 0.0001$) on the shear strength, with significantly higher values of shear strength for HO-derived biochars. No significant differences were detected between temperatures for this experiment (average values of 0.65 N mm^{-2} for VS, and 1.03 N mm^{-2} for HO).

Significant differences ($p = 0.031$) were detected between biochars produced from different biomass sources during the load tests conducted using the shear Kramer cell (see Figure 2c). HO-derived biochar supported higher levels of force (N) than VS-derived biochars. Selecting by feedstock, ANOVA revealed no significant differences between temperatures for this experiment (average values of 203.65 ± 0.69 and 204.68 ± 1.19 N for 400 and 600 °C, respectively). A significant effect was observed in this experiment for HO400, in which a significantly ($p = 0.001$) higher content of fine particles was collected after each experiment (average values of 0.027 ± 0.001 g for HO400 and 0.009 ± 0.002 g for HO600, respectively). This difference was not found between feedstocks and VS pyrolysis temperatures which presented an average value of 0.017 ± 0.01 g. Chrzazvez et al. [55] studied the fragmentation of different charcoal samples from tree species. They reported the higher level of fragmentation under compression forces for *Quercus* charcoal linked to the presence of a significant porous zone and a specific fragmentation mode of this species, which differs from others by the presence of multiseriate rays, related to the formation of fragile zones after combustion.

As mentioned above, the lignocellulosic composition of the biomass used as feedstock is of special interest in this study, since biochar usually keeps the morphological features of its feedstock after thermochemical conversion [41,56]. Wood pyrolysis commonly leads to a higher proportion of lignin than herbaceous biomasses, which usually have a higher cellulose content [41,57,58]. The lignocellulosic constituents degrade at different temperatures during the pyrolysis process (hemicellulose–complete starting at 330 °C; cellulose–greatest proportion degradation at 427 °C; lignin–complete degradation after 607 °C) [41,57–60]. The contents of lignin in the raw biomasses (see Table 1) were slightly higher for HO than for VS. This could explain the higher resistance of HO-derived biochars to impact strength. Nevertheless, the analyzed feedstocks have different bulk densities, which could also play a key role in determining the impact resistance and shear strength of HO-derived. This is in line with the results reported by Kumar et al. [37] and de Abreu Neto et al. [43], who observed a positive correlation between hardness and apparent density of wood chars. However, Dias Júnior et al. [38], in view on their breaking strength measurements for several charcoals produced at different pyrolysis temperatures, suggested that the apparent density of charcoal by itself was not a suitable indicator of its mechanical resistance.

With regard to the influence of temperature on mechanical strength, previous studies [37,42] reported a clear decrease in compressive/crushing/impact strength with in-

creasing carbonization temperature up to 500–600 °C. However, the results reported herein suggest that an increment in the final pyrolysis temperature from 400 °C to 600 °C led to a better mechanical behavior of biochar under specific forces. This finding seems to be consistent with the observations reported by Xie et al. [44], who observed a gradual increase in hardness with the pyrolysis temperature (in the range of 300–700 °C) for corn stalk pellets-derived biochars. Zickler et al. [56] also observed a continuous increase in the elastic modulus and hardness above 400 °C (via nanoindentation). Dias Júnior et al. [38] showed the same correlation in wood-derived charcoals. According to Das et al. [41], biochar made at temperature of around 450 °C presents a disintegrated micro-structure, exhibiting a defective structure of pyrolytic tars that lends to lower hardness. During the pyrolysis process, fragmentation and depolymerization occur, resulting in chemical degradation products that may have a certain effect on the final mechanical properties of the biochar [41]. This could be one of the reasons to explain the results from our study, in which lower average values of resistance were observed for VS400 (impact strength) and HO400 (shear strength), which exhibited higher contents of volatile matter (and, consequently, lower fixed-carbon contents) in comparison to VS600 and HO600 biochars (with more aromatic carbon structures). However, the above-explained effect of temperature was not statistically significant. The fact that the two types of biochar showed different behaviors under static and dynamic forces leads to the conclusion that feedstock nature plays an important role in determining the mechanical properties of resulting biochars.

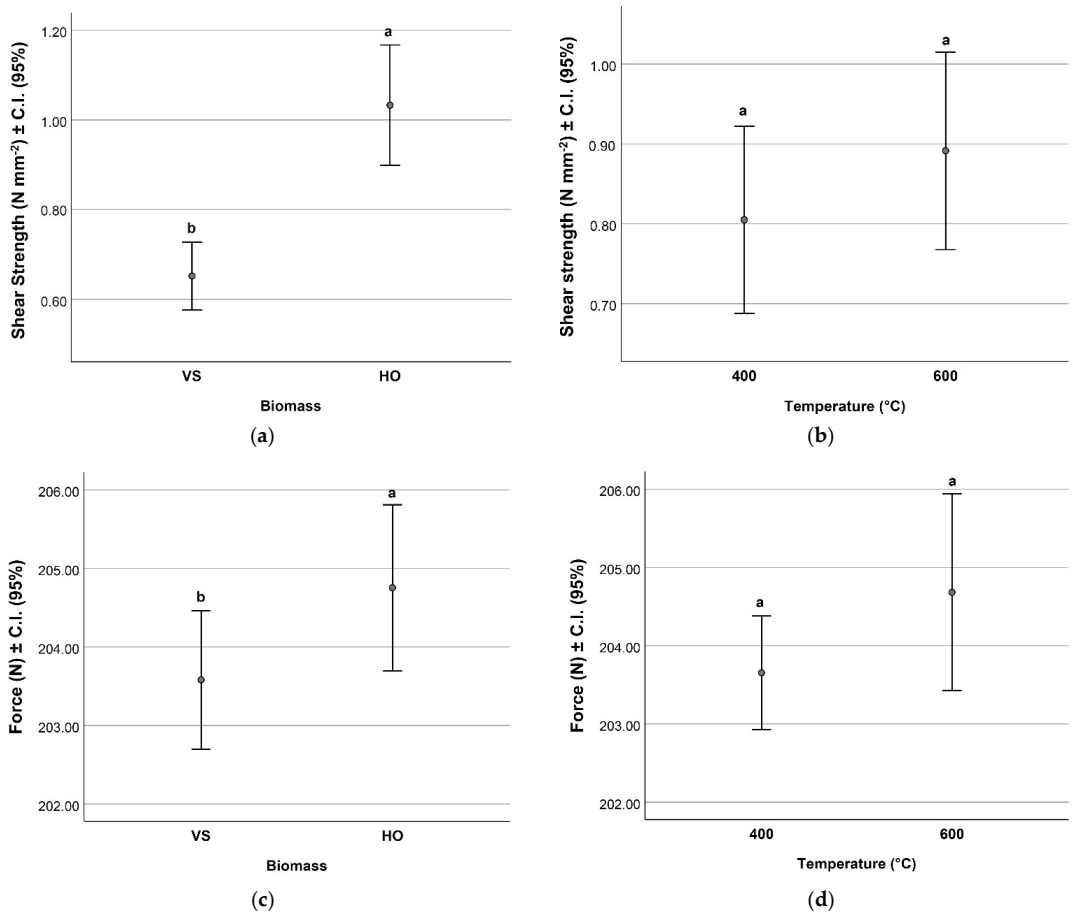

Figure 2. Effect of final pyrolysis temperature on: (**a**) shear strength as a function of biomass and (**b**) final pyrolysis temperature. (**c**) The breaking force supported into the Kramer shear cell as a function of biomass and (**d**) final pyrolysis temperature. VS: Vine Shoots; HO: Holm Oak; 400/600: final pyrolysis temperature-°C; different letters within a graph show statistically significant differences ($p < 0.05$).

3.3. Particle Size Distribution and Mechanical Processing

Table 4 details the *p*-value results from a three-way ANOVA performed to assess the influence of factors (i.e., biomass type, final pyrolysis temperature, and mechanical process) on the particle size distribution of biochar samples.

Table 4. Influence of biomass type, final pyrolysis temperature and process on the particle size distribution (mm).

Factor	≥20	2–20	0.250–2	0.125–0.250	0.090–0.125	0.010–0.090	<0.010
Biomass (B)		0.008	<0.0001	<0.0001			
Temperature (T)	<0.0001	<0.0001	<0.0001	<0.0001	0.033	0.003	
Process (P)	<0.0001	<0.0001	<0.0001	0.012		0.007	
B × T	<0.0001	<0.0001	0.001	<0.0001			
B × P	<0.0001	<0.0001	0.004	0.007		<0.0001	
T × P	<0.0001	<0.0001	0.001		0.009	0.043	
B × T × P	<0.0001	<0.0001	0.021				

The type of biomass did not have a significant effect on either the fraction of larger particles (≥20 mm) nor the finest fractions (<0.010–0.125 mm). Both the main effects and interactions were more significant for the coarser fractions (0.125–>20 mm). The fraction 0.090–0.125 mm was only significantly affected by temperature (as a main factor) as well as the interaction between temperature and process type. The fraction 0.010–90 mm was the finest fraction significantly affected by temperature and process type, and also by the interactions between biomass–process and temperature–process. In addition, the finest fraction (<0.010 mm) was not significantly affected.

Figure 3a,b illustrate the particle size distributions of the samples. Results from one-way ANOVA regarding the effect of process application are shown in order to facilitate the interpretation for the different fractions selecting by biomass. In Figure 3, fraction < 0.010–0.250 mm is clustered. In Figure 3c,d, the disaggregation of this fraction is specifically shown for each type of processed biochar.

The initial average values for the percentage of fragments between 2 and 20 mm were 1.24% and 1.18% for VS and HO, respectively. Biochar produced at 400 °C significantly increased this percentage after the mechanical processing for both feedstocks (24.18% for VS400 and 14.18% for HO400). Moistening significantly reduced this percentage in VS400 (16.20%). However, regarding HO400, the larger percentage of this fraction was measured under wet conditions (33.61%). In the processing of VS-derived biochar produced at 600 °C, it was observed a significant reduction of this fraction (2–20 mm) under wet conditions (55% with respect to the dry processing). In addition, a significant increase in the percentage of particles between 0.250–2 mm was observed for HO400 after the mechanical processing, regardless of the moisture content.

With respect to the clustered fraction (<0.250 mm), VS biochar did not show significant differences on its cumulative percentage. HO400P15, HO600P, and HO600P15 showed significant increases in this fraction, with particularities that are shown in Figure 3c,d.

The analysis of the particle size distribution below 0.250 mm is especially relevant, since fine particles can be dissolved into the atmosphere and lead to mass losses during the application process. In general, the particle size fraction below 0.250 mm was small, ranging from 0.09% (VS600) to 1.29% (HO400P15), in mass basis. As can be deduced from Figure 3c,d, HO biochars exhibited a more homogeneous behavior compared with VS biochars (the slightly significant differences are reported in the graphs with the purpose to provide useful information for future characterizations of VS and HO-derived biochars). In any case, the fine particle fractions reported herein are much lower than the percentage of mass losses (30%) measured by Blue Leaf Inc. during the application in field trials of a fine grained biochar produced by fast pyrolysis [18].

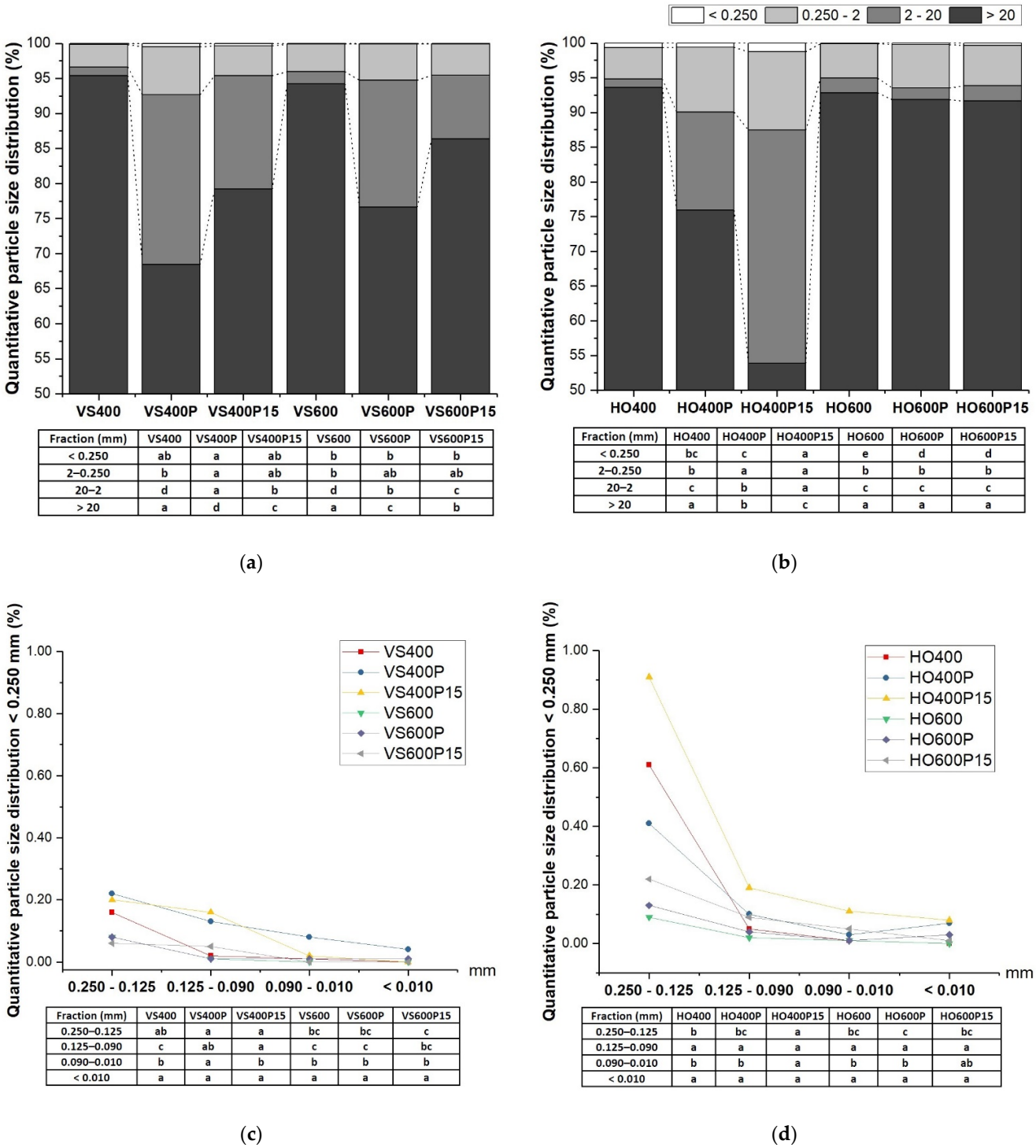

Figure 3. Quantitative particle size distribution (%): (**a**) VS- and (**b**) HO-derived biochar, both lower and larger size classes (mm) were considered; (**c**) VS- and (**d**) HO-derived biochar, the former smallest class (<0.250) was broken down into further classes. (VS/HO: Vine shoots/Holm Oak; 400/600: final pyrolysis temperature-°C; P: processed into the mechanical agitation system; P15: 15 wt.% moisture content; different letters within a row show significant differences at $p < 0.05$–Tukey´s test).

Moistening had a significant effect on particle size distribution, leading to a reduced fragmentation of coarse fractions in VS biochar; this could be attributed to an increase in compressive strength through the increased bonding and bridging between biochar particles in the presence of moisture as a result of enhanced Van der Waals forces, as it was

previously reported by Bazargan et al. [34]. Silva et al. [26] reported that 15 wt.% water content increased resistance to erodibility of larger particles due to weight gain by water absorption. For HO600 biochar, which appeared as the most homogeneous biochar, no significant variations were found between non-processed samples and processed under the two moisture contents. Conversely, HO400 showed again the lower resistance to mechanical stress, in line with the previous results reported for shear strength. For this biochar, moistening had the opposite effect to that expected, leading to an increase in fragmentation and thus in the fractions of fine particles. This finding could be ascribed to the heterogeneous structure of HO400 (in comparison with the more aromatic structure of HO600), as it has been aforementioned. On the other hand, the observed lower WHC of HO400 (4.56%) could also be related to its structure. In fact, this biochar did not retain the 15 wt.% of moisture applied before processing, suggesting that the disaggregation of fragments during mechanical processing was promoted by the high amount of free water in the mechanical agitation system.

Regarding PM_{10} fraction, the main percentages were higher for HO biochars than for VS biochars (with a maximum value of 0.08% for HO400P15). However, there was no statistically significant difference with respect to all the factors examined.

Biochar particle size is a key parameter that can affect the biological and physicochemical properties of the soil, which seem to be improved when relatively fine particles of biochar are used [13,14]. However, in order to determine the most appropriate biochar particle size it should also be considered aspects related to production, handling, and application systems, as well as ignition hazards and dust production issues. In this sense, the relatively large particle sizes tested in the present study was previously studied, and several benefits derived from its application were reported [46,61]. Considering the results obtained, the potential benefits of moistening biochar prior to the application depend on the final purpose and the type of biochar. Dust production and percolation of fine particulate matter should not be controlled at the application time focusing on a moisture content, since fragmentation is regulated by structural properties of biochar.

4. Conclusions

Results reported herein revealed that vine shoots and holm oak pruning residues can be considered as interesting biomass sources, whose management is suitable for the production of biochar. The physicochemical properties of resulting biochars were appropriate for agricultural purposes.

The mechanical behavior of these two types of biochar varied a lot depending on the application of static or dynamic forces: HO biochar exhibited higher impact strength than VS biochar, whose value could not be determined from a maximum height of 3 m. Final pyrolysis temperature did not significantly affect the impact strength resistance for VS. HO biochar showed higher resistance to shear strength and compression/shear combination forces than VS biochar. Final pyrolysis temperature did not significantly influence the resistance to static forces. Significant effects of biomass type, final pyrolysis temperature and mechanical process were observed on the particle size distribution and its fragmentation under systematic mechanical solicitations. Moistening practice could reduce the fragmentation in some types of biochar if WHC of biochar and mechanical properties are considered.

Author Contributions: Conceptualization, F.J.G.-R. and J.J.M.; methodology, F.J.G.-R., J.J.M., M.V. (María Videgain), B.D., E.C.C. and M.V. (Mariano Vidal); software, M.V. (María Videgain); validation, F.J.G.-R., J.J.M., M.V. (Mariano Vidal), B.D. and E.C.C.; formal analysis, J.J.M., F.J.G.-R., M.V. (María Videgain), B.D., E.C.C. and M.V. (Mariano Vidal); investigation, J.J.M., F.J.G.-R., M.V. (Mariano Vidal), B.D., E.C.C. and M.V. (María Videgain); resources, J.J.M., F.J.G.-R. and M.V. (María Videgain); data curation, J.J.M., F.J.G.-R. and M.V. (María Videgain); writing—original draft preparation, M.V. (María Videgain); writing—review and editing, F.J.G.-R., J.J.M., M.V. (Mariano Vidal), B.D. and E.C.C.; visualization, M.V. (María Videgain); supervision, F.J.G.-R., J.J.M., B.D. and E.C.C.; project

administration, J.J.M., F.J.G.-R. and M.V. (María Videgain); funding acquisition, J.J.M., F.J.G.-R. and M.V. (María Videgain). All authors have read and agreed to the published version of the manuscript.

Funding: This research received funding from the Spanish Ministry of Sciences, Innovation and Universities (ERANET-MED Project MEDWASTE, ref. PCIN-2017-048).

Institutional Review Board Statement: Not applicable.

Informed Consent Statement: Not applicable.

Data Availability Statement: The data presented in this article are available on request from the corresponding author.

Acknowledgments: The authors would like to acknowledge the collaboration and help given by students G. Greco and C. di Stasi (EPS), J. Moreno (EPS), P. Martín (EPS), S. García-Barreda (CITA), laboratory technicians of EPS–Universidad de Zaragoza and mechanic workshop technicians of LPF Tagralia.

Conflicts of Interest: The authors declare no conflict of interest.

References

1. International Biochar Initiative. Standardized Product Definition and Product Testing Guidelines for Biochar that Is Used in Soil. *Int. Biochar Initiat.* **2015**, *23*. Available online: https://www.biochar-international.org/wp-content/uploads/2018/04/IBI_Biochar_Standards_V2.1_Final.pdf (accessed on 9 October 2021).
2. Guo, M.; He, Z.; Uchimiya, S.M. Introduction to Biochar as an Agricultural and Environmental Amendment. In *Agricultural and Environmental Applications of Biochar: Advances and Barriers*; Guo, M., He, Z., Uchimiya, S.M., Eds.; Soil Science Society of America, Inc.: Madison, WI, USA, 2016; pp. 1–14.
3. Paz-Ferreiro, J.; Méndez, A.; Tarquis, A.M.; Cerdà, A.; Gascó, G. Preface: Environmental benefits of biochar. *Solid Earth* **2014**, *5*, 1301–1303. [CrossRef]
4. Ayaz, M.; Feizienė, D.; Tilvikienė, V.; Akhtar, K.; Stulpinaitė, U.; Iqbal, R. Biochar role in the sustainability of agriculture and environment. *Sustainability* **2021**, *13*, 1330. [CrossRef]
5. Khawkomol, S.; Neamchan, R.; Thongsamer, T.; Vinitnantharat, S.; Panpradit, B.; Sohsalam, P.; Werner, D.; Mrozik, W. Potential of biochar derived from agricultural residues for sustainable management. *Sustainability* **2021**, *13*, 8147. [CrossRef]
6. Blanco-Canqui, H. Does biochar improve all soil ecosystem services? *GCB Bioenergy* **2021**, *13*, 291–304. [CrossRef]
7. Hussain, R.; Garg, A.; Ravi, K. Soil-biochar-plant interaction: Differences from the perspective of engineered and agricultural soils. *Bull. Eng. Geol. Environ.* **2020**, *79*, 4461–4481. [CrossRef]
8. Yan, T.; Xue, J.; Zhou, Z.; Wu, Y. The trends in research on the effects of biochar on soil. *Sustainability* **2020**, *12*, 7810. [CrossRef]
9. Manyà, J.J.; Ortigosa, M.A.; Laguarta, S.; Manso, J.A. Experimental study on the effect of pyrolysis pressure, peak temperature, and particle size on the potential stability of vine shoots-derived biochar. *Fuel* **2014**, *133*, 163–172. [CrossRef]
10. Manyà, J.J.; Azuara, M.; Manso, J.A. Biochar production through slow pyrolysis of different biomass materials: Seeking the best operating conditions. *Biomass Bioenergy* **2018**, *117*, 115–123. [CrossRef]
11. Ahmad, J.; Vakalis, S.; Patuzzi, F.; Baratieri, M. Effect of process conditions on the surface properties of biomass chars produced by means of pyrolysis and CO_2 gasification. *Energy Environ.* **2020**. [CrossRef]
12. Gale, N.V.; Thomas, S.C. Dose-dependence of growth and ecophysiological responses of plants to biochar. *Sci. Total Environ.* **2019**, *658*, 1344–1354. [CrossRef]
13. De Jesus Duarte, S.; Glaser, B.; Cerri, C.E.P. Effect of biochar particle size on physical, hydrological and chemical properties of loamy and sandy tropical soils. *Agronomy* **2019**, *9*, 165. [CrossRef]
14. Liang, C.; Gascó, G.; Fu, S.; Méndez, A.; Paz-Ferreiro, J. Biochar from pruning residues as a soil amendment: Effects of pyrolysis temperature and particle size. *Soil Tillage Res.* **2016**, *164*, 3–10. [CrossRef]
15. Manyà, J.J. Pyrolysis for biochar purposes: A review to establish current knowledge gaps and research needs. *Environ. Sci. Technol.* **2012**, *46*, 7939–7954. [CrossRef] [PubMed]
16. Baveye, P.C. The Characterization of Pyrolysed Biomass Added to Soils Needs to Encompass Its Physical And Mechanical Properties. *Soil Sci. Soc. Am. J.* **2014**, *78*, 2112–2113. [CrossRef]
17. Schmidt, H. European Biochar Certificate (EBC)-guidelines version 6.1. *Biochar* **2015**. [CrossRef]
18. Major, J. *Guidelines on Practical Aspects of Biochar Application to Field Soil in Various Soil Management Systems*; International Biochar Initiative: Canandaigua, NY, USA, 2010. [CrossRef]
19. Liu, X.; Zhang, A.; Ji, C.; Joseph, S.; Bian, R.; Li, L.; Pan, G.; Paz-Ferreiro, J. Biochar's effect on crop productivity and the dependence on experimental conditions—A meta-analysis of literature data. *Plant Soil* **2013**, *373*, 583–594. [CrossRef]
20. Das, S.K.; Ghosh, G.K.; Avasthe, R. Application of biochar in agriculture and environment, and its safety issues. *Biomass Convers. Biorefinery* **2020**, 1–11. [CrossRef]
21. Sadasivam, B.Y.; Reddy, K.R. Engineering properties of waste wood-derived biochars and biochar-amended soils. *Int. J. Geotech. Eng.* **2015**, *9*, 521–535. [CrossRef]

22. Gelardi, D.L.; Li, C.; Parikh, S.J. An emerging environmental concern: Biochar-induced dust emissions and their potentially toxic properties. *Sci. Total Environ.* **2019**, *678*, 813–820. [CrossRef]
23. Li, C.; Bair, D.A.; Parikh, S.J. Estimating potential dust emissions from biochar amended soils under simulated tillage. *Sci. Total Environ.* **2018**, *625*, 1093–1101. [CrossRef] [PubMed]
24. Maienza, A.; Genesio, L.; Acciai, M.; Miglietta, F.; Pusceddu, E.; Vaccari, F.P. Impact of biochar formulation on the release of particulate matter and on short-term agronomic performance. *Sustainability* **2017**, *9*, 1131. [CrossRef]
25. Wang, D.; Zhang, W.; Hao, X.; Zhou, D. Transport of biochar particles in saturated granular media: Effects of pyrolysis temperature and particle size. *Environ. Sci. Technol.* **2013**, *47*, 821–828. [CrossRef] [PubMed]
26. Silva, F.C.; Borrego, C.; Keizer, J.J.; Amorim, J.H.; Verheijen, F.G.A. Effects of moisture content on wind erosion thresholds of biochar. *Atmos. Environ.* **2015**, *123*, 121–128. [CrossRef]
27. Busscher, W.J.; Novak, J.M.; Evans, D.E.; Watts, D.W.; Niandou, M.A.S.; Ahmedna, M. Influence of pecan biochar on physical properties of a Norfolk loamy sand. *Soil Sci.* **2010**, *175*, 10–14. [CrossRef]
28. Gümüş, İ.; Negiş, H.; Şeker, C. Influence of Biochar Applications on Modulus of Rupture and Aggregate Stability of the Soil Possessing Crusting Problems. *Toprak Su Derg.* **2019**, *8*, 81–86. [CrossRef]
29. Wani, I.; Ramola, S.; Garg, A.; Kushvaha, V. Critical review of biochar applications in geoengineering infrastructure: Moving beyond agricultural and environmental perspectives. *Biomass Convers. Biorefin.* **2021**. [CrossRef]
30. Xu, K.; Yang, B.; Wang, J.; Wu, M.Z. Improvement of mechanical properties of clay in landfill lines with biochar additive. *Arab. J. Geosci.* **2020**, *13*, 1–12. [CrossRef]
31. Yargicoglu, E.N.; Sadasivam, B.Y.; Reddy, K.R.; Spokas, K. Physical and chemical characterization of waste wood derived biochars. *Waste Manag.* **2015**, *36*, 256–268. [CrossRef]
32. Akinyemi, B.A.; Adesina, A. Recent advancements in the use of biochar for cementitious applications: A review. *J. Build. Eng.* **2020**, *32*, 101705. [CrossRef]
33. Azargohar, R.; Nanda, S.; Kang, K.; Bond, T.; Karunakaran, C.; Dalai, A.K.; Kozinski, J.A. Effects of bio-additives on the physicochemical properties and mechanical behavior of canola hull fuel pellets. *Renew. Energy* **2019**, *132*, 296–307. [CrossRef]
34. Bazargan, A.; Rough, S.L.; McKay, G. Compaction of palm kernel shell biochars for application as solid fuel. *Biomass Bioenergy* **2014**, *70*, 489–497. [CrossRef]
35. Hu, Q.; Shao, J.; Yang, H.; Yao, D.; Wang, X.; Chen, H. Effects of binders on the properties of bio-char pellets. *Appl. Energy* **2015**, *157*, 508–516. [CrossRef]
36. Assis, M.R.; Brancheriau, L.; Guibal, D.; Napoli, A.; Trugilho, P.F. Assis_2020_SpecificMethods.pdf. *BioResources* **2020**, *15*, 7660–7670.
37. Kumar, M.; Verma, B.B.; Gupta, R.C. Mechanical properties of acacia and eucalyptus wood chars. *Energy Sources* **1999**, *21*, 675–685. [CrossRef]
38. Dias Junior, A.F.; Esteves, R.P.; da Silva, Á.M.; Sousa Júnior, A.D.; Oliveira, M.P.; Brito, J.O.; Napoli, A.; Braga, B.M. Investigating the pyrolysis temperature to define the use of charcoal. *Eur. J. Wood Wood Prod.* **2020**, *78*, 193–204. [CrossRef]
39. de Abreu Neto, R.; Ramalho, F.M.G.; Costa, L.R.; Hein, P.R.G. Estimating hardness and density of wood and charcoal by near-infrared spectroscopy. *Wood Sci. Technol.* **2021**, *55*, 215–230. [CrossRef]
40. Winsley, P. Biochar and bioenergy production for climate change mitigation. *Sci. Technol.* **2007**, *64*, 5–10.
41. Das, O.; Sarmah, A.K.; Bhattacharyya, D. Structure-mechanics property relationship of waste derived biochars. *Sci. Total Environ.* **2015**, *538*, 611–620. [CrossRef]
42. Assis, M.R.; Brancheriau, L.; Napoli, A.; Trugilho, P.F. Factors affecting the mechanics of carbonized wood: Literature review. *Wood Sci. Technol.* **2016**, *50*, 519–536. [CrossRef]
43. de Abreu Neto, R.; De Assis, A.A.; Ballarin, A.W.; Hein, P.R.G. Dynamic Hardness of Charcoal Varies According to the Final Temperature of Carbonization. *Energy Fuels* **2018**, *32*, 9659–9665. [CrossRef]
44. Xie, R.; Zhu, Y.; Zhang, H.; Zhang, P.; Han, L. Effects and mechanism of pyrolysis temperature on physicochemical properties of corn stalk pellet biochar based on combined characterization approach of microcomputed tomography and chemical analysis. *Bioresour. Technol.* **2021**, *329*, 124907. [CrossRef]
45. de Abreu Neto, R.; de Assis, A.A.; Ballarin, A.W.; Hein, P.R.G. Effect of final temperature on charcoal stiffness and its correlation with wood density and hardness. *SN Appl. Sci.* **2020**, *2*, 1–9. [CrossRef]
46. Videgain-Marco, M.; Marco-Montori, P.; Martí-Dalmau, C.; Jaizme-Vega, M.D.C.; Manyà-Cervelló, J.J.; García-Ramos, F.J. Effects of Biochar Application in a Sorghum Crop under Greenhouse Conditions: Growth Parameters and Physicochemical Fertility. *Agronomy* **2020**, *10*, 104. [CrossRef]
47. Manyà, J.J.; Alvira, D.; Videgain, M.; Duman, G.; Yanik, J. Assessing the Importance of Pyrolysis Process Conditions and Feedstock Type on the Combustion Performance of Agricultural- Residue-Derived Chars. *Energy Fuels* **2021**, *35*, 3174–3185. [CrossRef]
48. American Standard of Testing Material: Standard Test Method for Chemical Analysis of Wood Charcoal ASTM D 1762-84 2001. Available online: https://www.astm.org/DATABASE.CART/HISTORICAL/D1762-84R01.htm (accessed on 9 October 2021).
49. Van Soest, P.J.; Robertson, J.B.; Lewis, B.A. Methods for Dietary Fiber, Neutral Detergent Fiber, and Nonstarch Polysaccharides in Relation to Animal Nutrition. *J. Dairy Sci.* **1991**, *74*, 3583–3597. [CrossRef]
50. Greco, G.; Di Stasi, C.; Rego, F.; González, B.; Manyà, J.J. Effects of slow-pyrolysis conditions on the products yields and properties and on exergy efficiency: A comprehensive assessment for wheat straw. *Appl. Energy* **2020**, *279*, 115842. [CrossRef]

51. Greco, G.; Videgain, M.; Di Stasi, C.; González, B.; Manyà, J.J. Evolution of the mass-loss rate during atmospheric and pressurized slow pyrolysis of wheat straw in a bench-scale reactor. *J. Anal. Appl. Pyrolysis* **2018**, *136*, 18–26. [CrossRef]
52. López-Cano, I.; Cayuela, M.L.; Mondini, C.; Takaya, C.A.; Ross, A.B.; Sánchez-Monedero, M.A. Suitability of different agricultural and urban organic wastes as feedstocks for the production of Biochar-Part 1: Physicochemical characterisation. *Sustainability* **2018**, *10*, 2265. [CrossRef]
53. Collard, F.X.; Blin, J. A review on pyrolysis of biomass constituents: Mechanisms and composition of the products obtained from the conversion of cellulose, hemicelluloses and lignin. *Renew. Sustain. Energy Rev.* **2014**, *38*, 594–608. [CrossRef]
54. Brewer, C.E.; Chuang, V.J.; Masiello, C.A.; Gonnermann, H.; Gao, X.; Dugan, B.; Driver, L.E.; Panzacchi, P.; Zygourakis, K.; Davies, C.A. New approaches to measuring biochar density and porosity. *Biomass Bioenergy* **2014**, *66*, 176–185. [CrossRef]
55. Chrzazvez, J.; Théry-Parisot, I.; Fiorucci, G.; Terral, J.F.; Thibaut, B. Impact of post-depositional processes on charcoal fragmentation and archaeobotanical implications: Experimental approach combining charcoal analysis and biomechanics. *J. Archaeol. Sci.* **2014**, *44*, 30–42. [CrossRef]
56. Zickler, G.A.; Schöberl, T.; Paris, O. Mechanical properties of pyrolysed wood: A nanoindentation study. *Philos. Mag.* **2006**, *86*, 1373–1386. [CrossRef]
57. Askeland, M.; Clarke, B.; Paz-Ferreiro, J. Comparative characterization of biochars produced at three selected pyrolysis temperatures from common woody and herbaceous waste streams. *PeerJ* **2019**, *7*, e6784. [CrossRef]
58. Azargohar, R.; Jacobson, K.L.; Powell, E.E.; Dalai, A.K. Evaluation of properties of fast pyrolysis products obtained, from Canadian waste biomass. *J. Anal. Appl. Pyrolysis* **2013**, *104*, 330–340. [CrossRef]
59. Yeo, J.Y.; Chin, B.L.F.; Tan, J.K.; Loh, Y.S. Comparative studies on the pyrolysis of cellulose, hemicellulose, and lignin based on combined kinetics. *J. Energy Inst.* **2019**, *92*, 27–37. [CrossRef]
60. Buss, W.; Mašek, O.; Graham, M.; Wüst, D. Inherent organic compounds in biochar-Their content, composition and potential toxic effects. *J. Environ. Manag.* **2015**, *156*, 150–157. [CrossRef] [PubMed]
61. Videgain-Marco, M.; Marco-Montori, P.; Martí-Dalmau, C.; Jaizme-Vega, M.C.; Manyà-Cervelló, J.J.; García-Ramos, F.J. The Effects of Biochar on Indigenous Arbuscular Mycorrhizae Fungi from Agroenvironments. *Plants* **2021**, *10*, 950. [CrossRef]